Periodic X-ray modulations in Supersoft X-ray Sources[1]

A Odendaal[1], PJ Meintjes[1], PA Charles[2] and AF Rajoelimanana[3,4]

[1]Department of Physics, University of the Free State, P.O. Box 339, Bloemfontein, 9300, South Africa
[2]School of Physics and Astronomy, Southampton University, Southampton SO17 1BJ
[3]South African Astronomical Observatory, P.O. Box 9, Observatory, 7935, South Africa
[4]Astrophysics, Cosmology and Gravity Centre (ACGC), University of Cape Town, Private Bag X3, Rondebosch, 7701, South Africa

E-mail: WinkA@ufs.ac.za

Abstract. The supersoft source CAL 83 is often considered to be the prototype of its class. We report the discovery of modulations at a period of ~ 67 s in X-ray data of CAL 83. This may be the spin period of a highly spun-up white dwarf. The supersoft source SMC 13 has an orbital period of ~ 4.1 h. SMC 13 was reported in the literature to exhibit orbital modulation in its X-ray flux, as inferred from its folded ROSAT light curve. We report the confirmation of this orbital modulation from three *Chandra* data sets, each providing continuous coverage of ~ 2.7 complete orbital cycles.

1. Introduction

Supersoft X-ray sources (SSS) form a highly luminous ($\sim 10^{36} - 10^{38}$ erg s^{-1}) class of objects that emit more than $\sim 90\%$ of their energy below 0.5 keV. SSS were first observed with the *Einstein X-ray Observatory* (Long et al. 1981, Seward and Mitchell 1981) and further discoveries by ROSAT established them as a distinct class of objects (Trümper et al. 1991). Typical effective temperatures range between $\sim 15 - 80$ eV (see Kahabka and van den Heuvel (2006) for a recent review on SSS).

It was shown by van den Heuvel et al. (1992) that the low effective temperatures and high luminosities of these sources can be explained by the nuclear burning of hydrogen on the surface of a white dwarf accreting material on the thermal time scale of the donor. The accretion rate required for steady nuclear burning is $\sim 10^{-7} M_{\odot}$ yr^{-1}, which can be sustained if the donor mass is comparable to or greater than the white dwarf mass (Paczyński 1971, Savonije 1983). Many SSS are also believed to contain accretion discs.

Recent analysis of archived data of the binary supersoft sources CAL 83 and SMC 13 showed strong modulations in the X-ray waveband. We report preliminary results of the timing analysis performed on these data, based on the results obtained during the M.Sc. research of Odendaal (2012).

[1] Based on observations obtained with XMM-Newton, an ESA science mission with instruments and contributions directly funded by ESA Member States and NASA, as well as observations from the *Chandra Data Archive*.

2. CAL 83 in the Large Magellanic Cloud

2.1. Observations and data calibration

CAL 83 has been observed by XMM-Newton several times from April 2000 to May 2009. The X-ray data were recorded with the three EPIC detectors (MOS1, MOS2 and PN) and the Reflection Grating Spectrometers (RGS). All the data sets were calibrated by following standard data reduction procedures with the XMM-Newton Science Analysis System, Version 11.0. The arrival times in the calibrated event files were corrected to the solar system barycentre (TDB system). From each calibrated event file, a light curve with a binning of 10 s was created from the source photons in the $0.15 - 2.5$ keV range.

2.2. Timing analysis

Each of the CAL 83 X-ray light curves were detrended by subtracting the mean and dividing by the standard deviation. The task SCARGLE in the Starlink PERIOD package[2] was subsequently utilized to create a periodogram from each detrended light curve.

A power peak near 15 mHz ($P \sim 67$ s) at a $\gtrsim 2\sigma$ level was found in the EPIC PN (the most sensitive of the five detectors) periodograms of six of the observations. These periodograms are shown in figure 1. The periodograms of the EPIC MOS exposures of some of these observations exhibit a very weak feature near ~ 67 s. The periodicity was not detected in the RGS periodograms.

The EPIC PN data of the six data sets exhibiting the periodicity were reanalysed by subdividing the longer data sets into shorter light curves and creating a similar Lomb-Scargle periodogram for each. The results from the segments exhibiting the periodicity are summarized in table 1. The error bars on the period values were determined by the intrinsic Fourier resolution of each periodogram, which gives an error of $P^2/2T$ to either side of each period peak, where P is the period, and T the total length of the light curve.

It is evident from table 1 that the detected period varies over a range of several seconds. The power of the peak is also highly variable for the different periodograms. No obvious correlation was found between the mean count rate and peak power, although it was noted that the period was not detected in data sets where the EPIC PN count rate was below 1 count/s.

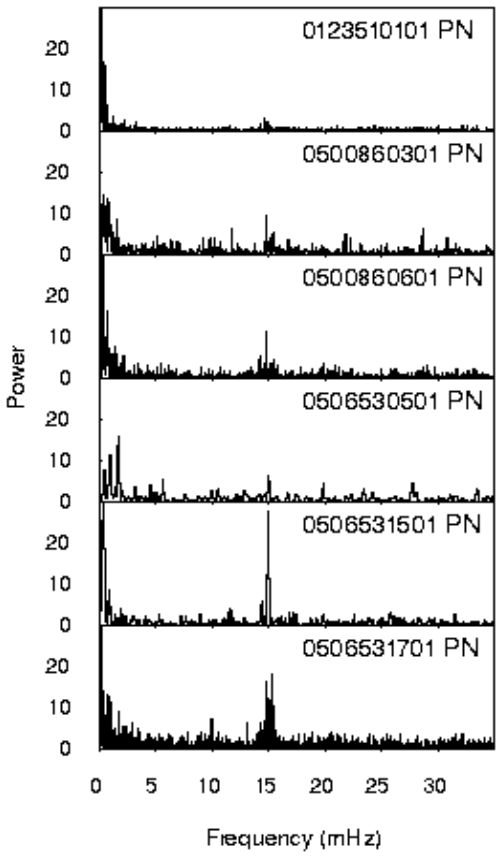

Figure 1. Lomb-Scargle periodograms of 6 EPIC PN observations exhibiting ~ 67 s periodicity.

2.3. Discussion

The exact origin of the ~ 67 s period is still under investigation. As the periodicity was found in the X-ray data, it is associated with the white dwarf. The fact that the modulation at ~ 67 s

[2] `http://www.starlink.rl.ac.uk/star/docs/sun167.htx/sun167.html`

Table 1. Timing analysis of the CAL 83 XMM-Newton PN light curves exhibiting a $\sim$ 67 s periodicity.

Obs ID	Length (s)	BJD (middle)	Period (s)	Peak power	Mean PN counts/s	Principal investigator
0123510101	5000	2451657.95459	68.591 ± 0.471	7.8	7.3	Fred Jansen
	5000	2451658.06917	67.891 ± 0.462	9.8	5.9	
	5000	2451658.12704	67.205 ± 0.453	5.2	6.7	
	5000	2451658.24162	67.205 ± 0.453	12.5	3.4	
	5000	2451658.29949	66.312 ± 0.441	7.7	3.0	
0500860301	5240	2454288.51696	64.969 ± 0.404	7.8	6.9	Thierry Lanz
	5240	2454288.57761	67.484 ± 0.435	8.6	6.8	
0500860601	5010	2454429.44780	67.797 ± 0.460	5.1	5.9	
	5010	2454429.56378	67.797 ± 0.460	9.3	6.9	
	5010	2454429.62176	69.930 ± 0.489	10.6	7.2	
0506530501	4600	2454573.12196	66.764 ± 0.486	6.6	2.1	Robert Schwarz
0506531501	6480	2454691.16206	66.873 ± 0.346	27.6	9.3	
0506531701	4570	2454981.86631	67.556 ± 0.500	7.8	8.8	
	4570	2454981.91920	66.569 ± 0.486	10.5	8.7	
	4570	2454981.97210	66.087 ± 0.479	15.9	9.2	
	4570	2454982.02499	64.911 ± 0.462	6.4	9.4	
	4570	2454982.07788	64.911 ± 0.462	5.5	7.9	
	4570	2454982.13078	67.306 ± 0.497	8.5	10.0	
	4570	2454982.18367	67.556 ± 0.500	4.7	9.8	
	4570	2454982.23657	66.087 ± 0.479	6.9	9.8	
	4570	2454982.28946	65.376 ± 0.469	15.6	8.9	
	4540	2454982.34224	65.324 ± 0.470	16.5	9.2	

is present in different data sets spanning over about 9 years possibly rules out short-lived quasi-periodic oscillations. A very promising possibility is that the periodicity represents the spin period of a magnetized white dwarf in CAL 83. The period is reminiscent of the short white dwarf spin periods in the cataclysmic variables AE Aqr ($\sim$ 33 s), V533 Her (63.633 s) and DQ Her (142 s) (Norton et al. 2004).

If it does represent the white dwarf spin period, one would expect the detected period to have exactly the same value in different data sets. However, it must be kept in mind that, although the arrival times have been corrected to the solar system barycentre, the orbital motion of the white dwarf will also modulate the detected spin period. This possibility is still under investigation.

Consistent modulations in other supersoft sources that have been ascribed to the spin period of a magnetized white dwarf are e.g. the 217.7 s pulsations in the source XMMU J004252.5+411540 in M31 (Trudolyubov and Priedhorsky 2008), and the 1110 s pulsations in Nova M31N 2007-12b (Pietsch et al. 2011). The recurrent nova RS Oph exhibited an unstable $\sim$ 35 s periodicity during the supersoft phase after its 2006 outburst (see Osborne et al. (2011) and references therein). The favoured explanation of this variable modulation is the possibility of non-radial oscillations caused by nuclear burning instabilities. It may be that the $\sim$ 67 s X-ray periodicity in CAL 83 is due to a similar effect.

3. SMC 13 in the Small Magellanic Cloud

An orbital ephemeris for SMC 13 was first determined by Schmidtke et al. (1994), who reported an orbital period of 0.1719 ± 0.0004 d, with minimum light at an epoch Nov. 3.105 1994. Kahabka

Table 2. Archived *Chandra* X-ray observations of SMC 13.

Obs ID	Instrument	Start date & time (UT)	Exposure time (s)	PI
4535	ACIS-S3	2005-01-30 16:56:17	40 140	J. Greiner
7456	HRC-S+LETG	2007-02-12 18:25:16	40 190	T. Lanz
8519	HRC-S+LETG	2007-02-18 00:42:08	42 670	T. Lanz

(1995) reported the discovery of orbital modulation in the ROSAT data of SMC 13, and Kahabka (1996) determined the ROSAT period to be 4.123 h (0.1718 d).

The orbital ephemeris of Schmidtke et al. (1994) was refined by Schmidtke et al. (1996) and Crampton et al. (1997), and additional photometric observations lead van Teeseling et al. (1998) to a revised orbital ephemeris of

$$T_0 = \text{HJD } 2450434.1320 \pm 0.0006 \quad + \quad 0.1719260E \pm 0.0000007 \text{ d} .$$

3.1. Observations and data calibration

Three archived *Chandra* observations of SMC 13 will be discussed, and these are summarized in table 2. The calibration of the data was carried out by following standard data reduction and processing procedures with the CIAO software, Version 4.3, using Version 4.4.5 of the CALDB (CIAO Calibration Database). The arrival times in the calibrated event files of the three observations were corrected to the solar system barycentre (TDB system).

3.2. Timing analysis

The PERIOD task SCARGLE was used to search for an orbital period in the *Chandra* X-ray light curves around the period of 4.123 h found by Kahabka (1996) in the ROSAT data. Each of the three Lomb-Scargle periodograms exhibited a strong power peak at the approximate position of the orbital period. However, the uncertainty in the peak positions was very high due to the relatively short length of the individual data sets. Therefore the X-ray modulation could be constrained to nothing better than 4.44 ± 0.89 h with the separate observations.

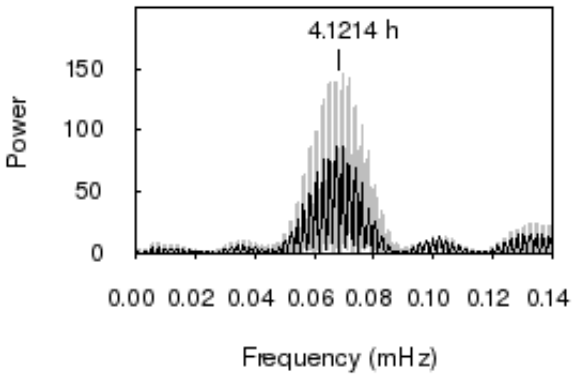

Figure 2. Lomb-Scargle periodograms of combined SMC 13 *Chandra* light curves. Black: Obs 7456 and 8519. Gray: Obs 4535, 7456 and 8519. The chosen peak at 4.1214 ± 0.0005 h is indicated.

To obtain a higher period resolution, two additional Lomb-Scargle periodograms were created (see figure 2): one by combining all three observations, and the other by combining only the observations of February 2007 (Obs 7456 and 8519). The strongest peak in the 2007 periodogram was determined to be at a period of 4.12 ± 0.06 h. The position of this (relatively broad) peak was then used to choose the appropriate peak on the high time-resolution periodogram obtained by combining all three data sets, yielding a final period of 4.1214 ± 0.0005 h.

The ROSAT light curves of Kahabka (1996) in the soft ($0.1 - 0.25$ keV) and hard ($0.26 - 0.50$ keV) energy bands, as well as the hardness ratio, folded on the ephemeris of Schmidtke et al. (1994) are shown in figure 3. As pointed out by Kahabka (1996), there seems to be a second dip

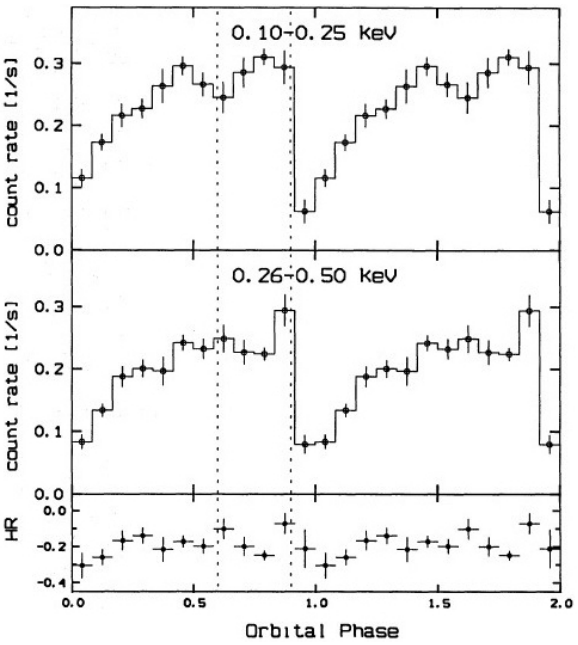

Figure 3. ROSAT light curves of SMC 13, folded on 4.123 h with respect to the epoch Nov. 3.105, 1994. The hardness ratio is HR=(H–S)/(H+S), where S is the number of counts in the soft band and H the number of counts in the hard band. (Adopted from Kahabka (1996, figure 3).)

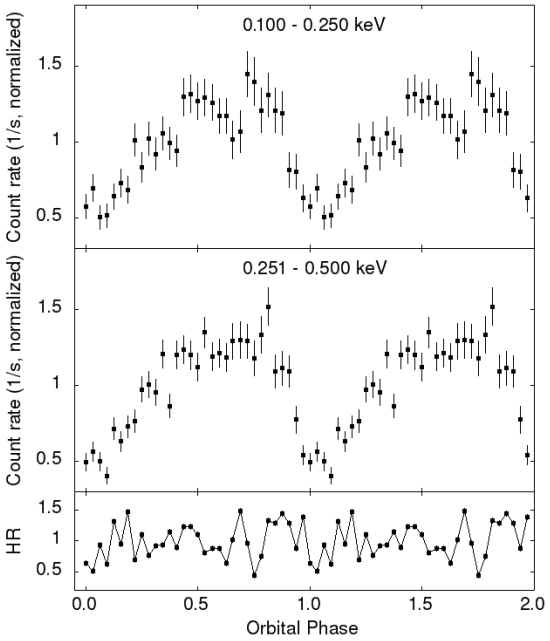

Figure 4. *Chandra* ACIS light curves of SMC 13, folded on $P_{\rm orb} = 4.1214$ h with respect to the third minimum in the data set. The hardness ratio is HR=H/(H+S), where H and S are the number of counts above and below 0.5 keV respectively.

at $\phi = 0.6$ in the $0.1 - 0.25$ keV band in addition to the main minimum at $\phi \sim 0.9 - 1.1$, and both the major and minors dips are coupled with an increase in the hardness ratio. It is also interesting to note that the count rate in the hard energy band correlates with the variations in HR.

The intrinsic energy resolution of the ACIS-S detector was used to create two similar *Chandra* light curves: one in the soft band ($0.100 - 0.250$ keV) and one in the hard band ($0.251 - 0.500$ keV). However, the hardness ratio was calculated in a different way than the ROSAT hardness ratio, in order to suit better the detectable energy range of SMC 13 covered by *Chandra*. The hardness ratio was defined as HR=H/(H+S), where H and S are the number of counts above and below 0.5 keV respectively. The soft, hard and HR light curves of observation 4535 were folded on the newly determined period by making use of the task **efold** in the Xronos Timing Analysis Software Package[3], using the time of minimum light of the third minimum of the Obs 4535 light curve (BJD 2453401.5682), and these are provided in figure 4.

3.3. Discussion

Because the time of minimum in the ROSAT light curve is largely defined by only three data points, Crampton et al. (1997) mentioned the possibility that these few minima might be caused by the system being in a low state at some epochs, rather than by orbital modulation. However, each of the *Chandra* data sets constitutes an uninterrupted observation of the source for a duration of ~ 2.7 full orbital periods, and the orbital modulation is clearly evident. As suggested

[3] See the Xronos User's Guide (HEASARC 2009) for more information.

by Kahabka (1996), the shape of the X-ray light curve may indicate that the WD possesses a substantial magnetic field.

The orbital period of 4.1214 ± 0.0005 h determined from the combined data set is very close to $P_{\rm orb} = 4.126224 \pm 0.000017$ h determined by van Teeseling et al. (1998), although not included in its error ranges.

Comparison of the folded ROSAT and *Chandra* light curves in figure 3 and figure 4 shows that they exhibit the same sharp, asymmetric form. The soft bands both show a shallow secondary minimum between phase values of 0.6 and 0.7, which is not observed in the hard bands. The HR values can not be compared directly, as they were defined differently. In the ROSAT light curve, both the minor and major dips are coupled with an increase in the hardness ratio. The trend of the HR to increase during the secondary minimum in the soft band is also observed in the *Chandra* data. However, the relative value of the *Chandra* HR is quite low during the main minimum.

From figure 3, it appears that the X-ray modulation is in phase with the orbital motion. On the other hand, Schmidtke et al. (1996) found that the X-ray minimum occurs about 0.25 of an orbital cycle later than the optical minimum, according to their ephemeris. However, folding the *Chandra* light curves through the orbital ephemeris of van Teeseling et al. (1998) showed that the X-ray minima approximately coincides with the optical minimum. Therefore a more in-depth analysis of the orbital period and ephemeris in conjunction with previous observations of SMC 13 needs to be carried out. In particular, simultaneous optical and X-ray observations are needed to clarify the relative phasing of the minima in these wavebands.

Acknowledgments

The financial assistance of the South African Square Kilometre Array Project towards this research is hereby acknowledged. Opinions expressed and conclusions arrived at, are those of the author and are not necessarily to be attributed to the NRF. We would like to thank the principal investigators of the archived X-ray data for the opportunity to analyse the data, as well as Frank Haberl for his comments on the periodicity detected in CAL 83.

References

Crampton D, Hutchings J B, Cowley A P and Schmidtke P C 1997 *ApJ* **489**, 903–11.

HEASARC 2009 *Xronos: A Timing Analysis Software Package. User's Guide Version 5.22.* Available at: `http://heasarc.gsfc.nasa.gov/docs/xanadu/xronos/`.

Kahabka P 1995 *in* H. Böhringer et al, ed., 'Seventeenth Texas Symposium on Relativistic Astrophysics and Cosmology' Vol. 759 of *Annals of the New York Academy of Sciences* p. 324.

Kahabka P 1996 *A&A* **306**, 795–802.

Kahabka P and van den Heuvel E P J 2006 Cambridge University Press New York chapter 11, pp. 461–74.

Long K S, Helfand D J and Grabelsky D A 1981 *ApJ* **248**, 925–44.

Norton A J, Wynn G A and Somerscales R V 2004 *ApJ* **614**, 349–57.

Odendaal A 2012 A Multi-Wavelength Study of Super Soft X-ray Sources in the Magellanic Clouds Master's thesis University of the Free State Bloemfontein.

Osborne J P et al. 2011 *ApJ* **727**, 124–33.

Paczyński B 1971 *ARA&A* **9**, 183–208.

Pietsch W, Henze M, Haberl F, Hernanz M, Sala G, Hartmann D H and Della Valle M 2011 *A&A* **531**, A22.

Savonije J 1983 *in* W. H. G. Lewin & E. P. J. van den Heuvel, ed., 'Accretion-Driven Stellar X-ray Sources' pp. 343–66.

Schmidtke P C, Cowley A P, McGrath T K, Hutchings J B and Crampton D 1994 *IAU Circulars* **6107**, 1.

Schmidtke P C, Cowley A P, McGrath T K, Hutchings J B and Crampton D 1996 *AJ* **111**, 788–93.

Seward F D and Mitchell M 1981 *ApJ* **243**, 736–43.

Trudolyubov S P and Priedhorsky W C 2008 *ApJ* **676**, 1218–25.

Trümper J et al. 1991 *Nature* **349**, 579–83.

van den Heuvel E P J, Bhattacharya D, Nomoto K and Rappaport S A 1992 *A&A* **262**, 97–105.

van Teeseling A, Reinsch K, Pakull M W and Beuermann K 1998 *A&A* **338**, 947–56.